Insights into the kinetics of siRNA-mediated gene silencing from live-cell and live-animal bioluminescent imaging

Derek W. Bartlett and Mark E. Davis*

Chemical Engineering, California Institute of Technology, Pasadena, CA 91125, USA

ABSTRACT

Small interfering RNA (siRNA) molecules are potent effectors of post-transcriptional gene silencing. Using noninvasive bioluminescent imaging and a mathematical model of siRNA delivery and function, the effects of target-specific and treatment-specific parameters on siRNA-mediated gene silencing are monitored in cells stably expressing the firefly luciferase protein. *In vitro*, luciferase protein levels recover to pre-treatment values within <1 week in rapidly dividing cell lines, but take longer than 3 weeks to return to steady-state levels in nondividing fibroblasts. Similar results are observed *in vivo*, with knockdown lasting ∼10 days in subcutaneous tumors in A/J mice and 3–4 weeks in the nondividing hepatocytes of BALB/c mice. These data indicate that dilution due to cell division, and not intracellular siRNA half-life, governs the duration of gene silencing under these conditions. To demonstrate the practical use of the model in treatment design, model calculations are used to predict the dosing schedule required to maintain persistent silencing of target proteins with different half-lives in rapidly dividing or nondividing cells. The approach of bioluminescent imaging combined with mathematical modeling provides useful insights into siRNA function and may help expedite the translation of siRNA into clinically relevant therapeutics for disease treatment and management.

INTRODUCTION

RNA interference (RNAi) refers to the ability of double-stranded RNA (dsRNA) to cause sequence-specific degradation of complementary mRNA molecules. Since its discovery in *Caenorhabditis elegans* in 1998 (1), it has rapidly attracted attention from researchers in fields ranging from genetics to clinical medicine. A natural intracellular process likely involved in cell-based defense against mobile genetic elements such as viruses and transposons (2), RNAi promises to be an invaluable tool for gene function analysis as well as a powerful therapeutic agent that can be used to silence pathogenic gene products associated with diseases including cancer, viral infections and autoimmune disorders (3–8).

A central component of RNAi is a double-stranded siRNA molecule that is 21–23 nt in length with 2 nt long 3′ overhangs (9). These siRNA effector molecules can be introduced into cells directly as synthetic siRNAs or indirectly as precursor long dsRNAs or short-hairpin RNAs (shRNAs). RNA polymerase II- or III-driven expression cassettes can be used for constitutive expression of shRNA molecules (10). Both the long dsRNAs and shRNAs are cleaved by Dicer (RNase III family of endonucleases) into the appropriately sized siRNA effectors. Although the presence of dsRNA >30 nt can elicit an interferon response in mammalian cells (11), Elbashir and co-workers demonstrated that synthetic 21mer siRNAs evaded the interferon response and yet were still effective mediators of sequence-specific gene silencing in mammalian cells (9). Here, we have chosen to focus on the use of synthetic 21mer siRNA duplex molecules in mammalian cells for transient gene silencing.

Because synthetic siRNA molecules must be transported into the cells before they can function in RNAi, successful delivery of siRNA is of central importance. Delivery vehicles must protect the siRNA from nucleases in the serum or extracellular media, enhance siRNA transport across the cell membrane and guide the siRNA to its proper location through interactions with the intracellular trafficking machinery. While naked siRNA molecules have been shown to enter cells, significantly more siRNA can be delivered using carrier vehicles (12,13). Both viral and nonviral vectors deliver siRNA into cells, although viral vectors are limited to

---

*To whom correspondence should be addressed. Tel: +1 626 395 4251; Fax: +1 626 568 8743; Email: mdavis@cheme.caltech.edu

delivering siRNA-expressing constructs such as shRNA. Commercially available cationic lipids such as Oligofectamine can effectively deliver siRNA molecules into cells *in vitro* with transfection efficiencies approaching 90% (9). However, the high toxicity of cationic lipids limits their use for systemic delivery *in vivo*. Recent studies from our laboratory have shown that cyclodextrin-containing polycations (CDPs) can achieve safe and effective systemic delivery of siRNA in mice (14). Here, we consider the nonviral delivery of siRNA using cationic lipids or polymers.

A challenge for the successful application of siRNA will be to determine the dosing schedule required for efficacy, making insights into the kinetics of siRNA-mediated gene silencing foundational for the future clinical use of siRNA. Without a proper understanding of the kinetics of the process and the parameters that can affect the resulting gene silencing, application of RNAi will be governed largely by trial and error. The ability to specifically tailor and optimize the treatment for each particular system would save significant time and resources, especially given the high cost of synthetic siRNA molecules and the amount of material required for *in vivo* studies. Mathematical modeling using simple kinetic equations for each step in the RNAi process can shed light on many of these questions regarding the kinetic aspects of RNAi. To our knowledge, there are only a few published examples of such studies looking at the kinetics of the intracellular RNAi process (15–18). Of these studies, none has combined the delivery process and the interaction with the RNAi machinery in mammalian cells. Bergstrom and co-workers (15) proposed a unidirectional amplification method in their mathematical model of RNAi-mediated gene silencing. Because no RNA-dependent RNA polymerase has yet been found in mammalian cells, they acknowledged that their model did not address the silencing mechanisms observed in mammals. Groenenboom and co-workers (16) recently proposed a mathematical model for RNAi that contained several extensions to the core RNAi pathway, providing for siRNA degradation by RNase as well as primed amplification. Their model aimed to explain transgene- or virus-induced gene silencing and avoidance of self-reactivity, but did not consider any steps in the delivery process. Similarly, Raab and Stephanopoulos (17) looked at the dynamics of gene silencing by siRNA given at different doses and at various times relative to plasmid transfection, but did not incorporate siRNA delivery. Arciero and co-workers (18) created a mathematical model to investigate tumor-immune evasion and siRNA treatment. Although this model provided insights into how siRNA can be used in cancer treatment, it did not examine the delivery process and there were no experimental data from *in vitro* or *in vivo* studies. Here, we use bioluminescent imaging and mathematical modeling to investigate the steps of RNAi from siRNA delivery to intracellular function with the aim of enabling the practical application and design of siRNA-based treatment strategies both *in vitro* and *in vivo*. Because the imaging is noninvasive and nondestructive, the same set of cells or animals can be followed for the entire study. These results will complement investigations using more traditional analytical methods to monitor mRNA or protein knockdown and hopefully serve to encourage the rational design of experimental and clinical siRNA-based treatments.

MATERIALS AND METHODS

Production of luciferase-expressing cell lines by lentiviral transduction

Cell lines were incubated with viral supernatant containing SMPU-R-MNCU3-LUC, a lentiviral vector based on HIV-1 that transduces the firefly luciferase gene. The backbone vector SMPU-R has deletions of the enhancers and promoters of the HIV-1 long terminal repeat (SIN), has minimal HIV-1 gag sequences, contains the cPPT/CTS sequence from HIV-1, has three copies of the UES polyadenylation enhancement element from SV40 and has a minimal HIV-1 RRE [gift from Paula Cannon, Children's Hospital Los Angeles, Los Angeles, CA (19)]. The vector has the U3 region from the MND retroviral vector as an internal promoter driving expression of the firefly luciferase gene from SP-LUC+ [Promega, Madison, WI (20)].

siRNA duplexes

All siRNA molecules were ordered purified and pre-annealed ('Option C') from Dharmacon Research, Inc. (Lafayette, CO). siGL3 (sense, 5′-CUUACGCUGAGUACUUCGAdTdT-3′; antisense, 5′-UCGAAGUACUCAGCGUAAGdTdT-3′) is an unmodified siRNA duplex that targets the luciferase gene, while siCONTROL non-targeting siRNA #1 (siCON1; sense, 5′-UAGCGACUAAACACAUCAAUU-3′; antisense, 5′-UUG-AUGUGUUUAGUCGCUAUU-3′) is an unmodified siRNA duplex bioinformatically designed to minimize the potential for targeting any known human or mouse genes.

In vitro transfections

Cells were seeded in 24-well plates 2–3 days prior to transfection at 2×10^4–1×10^5 cells per well and grown in media supplemented with 10% fetal bovine serum (FBS) and antibiotics (penicillin/streptomycin). siRNA was complexed with Oligofectamine (Invitrogen, Carlsbad, CA) according to the manufacturer's instructions and applied to each well in a total volume of 200 µl OptiMEM (Invitrogen). Transfection medium was removed and replaced with complete medium after 5 h.

Formation of subcutaneous tumors in mice

Luciferase-expressing Neuro2A (Neuro2A-Luc) cells were grown to confluence in media supplemented with 10% FBS and antibiotics (penicillin/streptomycin). Immediately prior to injection, cells were washed with phosphate-buffered saline (PBS), trypsinized and resuspended in serum-free media at 2×10^6 cells/ml. Each mouse received 0.5 ml of the resulting cell suspension by subcutaneous injection.

Low-pressure tail-vein (LPTV) injection of formulated siRNA polyplexes

All complexes were made with siRNA and an imidazole-modified CDP (CDP-Im) synthesized as described previously (21,22). Before addition to siRNA, CDP-Im was mixed with an adamantane-PEG$_{5000}$ (AD-PEG) conjugate and an AD-PEG-transferrin (Tf) conjugate such that the total moles of AD-PEG or AD-PEG-Tf equaled the number of moles of β-CD. Tf-targeted polyplexes contained 1% AD-PEG-Tf relative to AD-PEG. This mixture was added to an equal volume
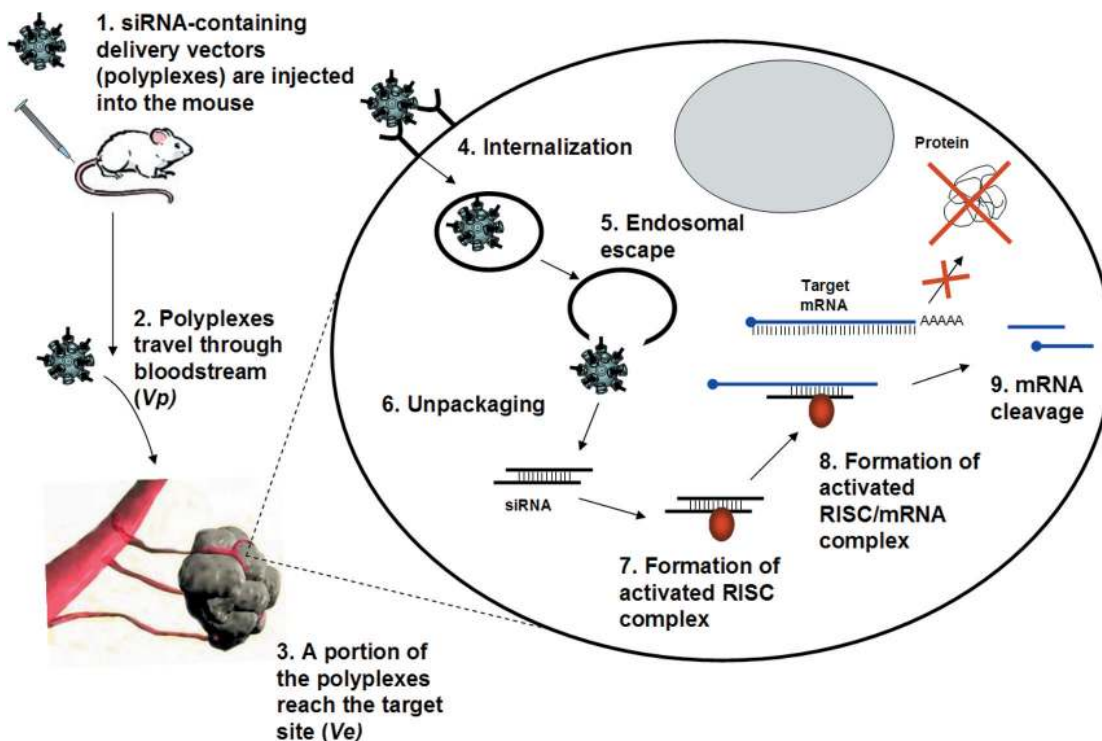
Figure 1. Simplified schematic of the key steps required for siRNA delivery to and function within mammalian cells. Steps 1–3 are unique to *in vivo* application of siRNA, whereas steps 4–9 represent the general processes on the level of an individual cell and are therefore common to both *in vivo* and *in vitro* application of siRNA.

of siRNA at a charge ratio (positive charges from CDP-Im to negative charges from siRNA backbone) of 3:1 (+:−). An equal volume of 10% (w/v) glucose in water was added to the resulting polyplexes to yield a 5% (w/v) glucose (D5W) solution suitable for injection. Each mouse was injected with 200 μl of this polyplex solution containing 50 μg siRNA per 20 g mouse (2.5 mg/kg siRNA).

High-pressure tail-vein (HPTV) co-injection of plasmid and siRNA

Hydrodynamic, or HPTV, injection of nucleic acids can achieve significant levels of nucleic acid in the hepatocytes of mice (23,24). A. McCaffrey and M. Kay kindly donated a plasmid (pApoEHCRLuc) containing the firefly luciferase gene under the control of the human α_1-antitrypsin promoter and the apolipoprotein E locus control region. For HPTV co-injection studies in BALB/c mice, each 20 g mouse received a 10% w/v injection of a D5W solution containing 0.25 mg/kg of the luciferase-containing plasmid and 2.5 mg/kg siRNA.

Bioluminescent imaging

Cell culture plates or mice containing the luciferase-expressing cells were imaged using the Xenogen IVIS 100 Imaging System (Xenogen, Alameda, CA). D-luciferin (Xenogen) was dissolved in PBS at 15 g/l. For *in vitro* assays in 24-well plates, 50 μl of the 15 g/l luciferin solution was added to each well containing 1 ml of media. Light emission was measured 2–3 min after addition of the luciferin. For *in vivo* experiments, 0.2 ml of the 15 g/l luciferin solution was injected intraperitoneally 10 min before measuring the

light emission. Mice were anesthetized with an initial dose of 5% isoflurane followed by a maintenance dose of 2.5% isoflurane. Bioluminescent signal intensities were quantified using Living Image software (Xenogen).

Mathematical model

The model presented here was designed to allow the user to specifically study the impact of parameter values on gene silencing by RNAi. When designing an siRNA-based treatment, the main controllable parameters are the delivery method (naked siRNA, formulated with vector, chemically modified) and dosing schedule. These choices must be governed by parameters such as the target mRNA half-life, target protein half-life, threshold for reduction (in either target mRNA or protein), number of target cells and desired knockdown duration. The model's design criteria therefore included the ability to enable user-defined values for these parameters that characterize each experimental system.

A simplified schematic of the major processes included in the model is shown in Figure 1. Model variables (Table 1) and parameters (Table 2) were used to develop a set of ordinary differential equations for the steps involved in siRNA delivery to and function within mammalian cells *in vitro* and *in vivo*. The differential equations governing each major process from the delivery of siRNA to its intracellular interaction with the RNAi machinery are grouped into modules that can be changed independently to modify the model complexity as desired. A detailed description of the mathematical model and the rationale for its design are provided in the Supplementary Data.

Table 1. Model variables

Name	Model compartment	Description (units)
Bcf	Plasma	Free complex in circulation (# vol^{-1})
Bcb	Plasma	Bound complex in circulation (# vol^{-1})
Ec	Extracellular	Extracellular complex in local vicinity (# vol^{-1})
Enc	Intracellular	Endosomal complex (# vol^{-1})
$Enna$	Intracellular	Endosomal free siRNA (# vol^{-1})
Cc	Intracellular	Cytoplasmic complex (# vol^{-1})
Cna	Intracellular	Cytoplasmic free siRNA (# vol^{-1})
R	Intracellular	Activated RISC complex (# vol^{-1})
C	Intracellular	Activated RISC complex bound to mRNA (# vol^{-1})
M	Intracellular	Target mRNA (# vol^{-1})
P	Intracellular	Target protein (# vol^{-1})
Z	Intracellular	Number of cells (#)

Circulation/extracellular transport

$$\frac{dBcf}{dt} = kblooddis \cdot Bcb - kbloodbind \cdot Bcf$$
$$- ktransblood \cdot partition \cdot Bcf - kelimpl \cdot Bcf$$

$$\frac{dBcb}{dt} = kbloodbind \cdot Bcf - kblooddis \cdot Bcb$$

$$\frac{dEc}{dt} = ktransblood \cdot partition \cdot \frac{Vp}{Ve} \cdot Bcf$$
$$- kint \cdot Ec \cdot Z - kelimec \cdot Ec$$

Cellular uptake and intracellular trafficking

$$\frac{dEnc}{dt} = kint \cdot \frac{Ve}{Vi} \cdot Ec \cdot - kescendvec \cdot Enc$$
$$- kunpackend \cdot Enc - dilution \cdot Enc$$

$$\frac{dEnna}{dt} = kunpackend \cdot Enc - kescendna \cdot Enna$$
$$- kdegendna \cdot Enna - dilution \cdot Enna$$

$$\frac{dCc}{dt} = kescendvec \cdot Enc - kunpackcyt \cdot Cc - dilution \cdot Cc$$

$$\frac{dCna}{dt} = kescendna \cdot Enna + kunpackcyt \cdot Cc + kdisRISC \cdot R$$
$$- kformRISC \cdot (rtot - R - C) \cdot Cna$$
$$- kdeginna \cdot Cna - dilution \cdot Cna$$

RNAi

$$\frac{dR}{dt} = kformRISC \cdot (rtot - R - C) \cdot Cna + kdisRISCm \cdot C$$
$$+ kcleavage \cdot C - kdisRISC \cdot R - kdegRISC \cdot (R + C)$$
$$- kformRISCm \cdot R \cdot M - dilution \cdot R$$

$$\frac{dC}{dt} = kformRISCm \cdot R \cdot M - kdisRISCm \cdot C$$
$$- kdegRISC \cdot (R + C) - kcleavage \cdot C - dilution \cdot C$$

$$\frac{dM}{dt} = kformmRNA + kdisRISCm \cdot C - kdegmRNA \cdot M$$
$$- kformRISCm \cdot R \cdot M$$

Cell growth and target protein production

$$\frac{dP}{dt} = kformprot \cdot M - kdegprot \cdot P$$

$$\frac{dZ}{dt} = kgrowth \cdot Z \cdot \left(1 - \frac{Z}{max}\right)$$

All of the equations for intracellular siRNA-associated species contain a term to account for dilution due to cell division, where dilution is equal to the ratio of new cells divided by the total number of cells. For example, if the number of cells doubles in 1 day, then dilution would equal 0.5 and the concentration of the intracellular species would likewise be reduced by 50%. For the sake of calculation simplicity, only species involving the delivered siRNA molecules are diluted by this factor; all other intracellular species (i.e. target mRNA and target protein) are assumed to not change after cell division because they are produced intracellularly by both of the daughter cells. The net effect of this is that the siRNA-associated species are diluted equally between the two daughter cells after each cell division.

The set of ODEs was solved with MATLAB (The MathWorks, Inc., Natick, MA) using the stiff ODE15s solver. The ODE15s solver is a variable-order solver based on the numerical differentiation formulas. Parametric sensitivity analysis was performed using SENS_SYS written by V. M. Garcia Molla. This MATLAB routine is an extension to the ODE15s solver that calculates the derivatives of the solution with respect to the parameters.

RESULTS

In vitro and *in vivo* experiments were conducted to gain insights into the general kinetics of siRNA-mediated gene silencing in cell lines that constitutively express the luciferase gene. Constitutively expressed genes, in contrast to genes expressed transiently by plasmids, provide a more realistic model for clinical application in which an endogenous gene, such as an oncogene, is the target for a therapeutic siRNA. The Xenogen IVIS 100 Imaging System allowed us to monitor luciferase activity in luciferase-expressing cells growing in 24-well plates or present in subcutaneous tumors or livers in live mice; because the imaging was noninvasive, luciferase activity was measured in the same plate of cells or the same animals over the entire duration of the study. Monitoring the kinetics of siRNA-mediated gene silencing in the same population of cells helps to avoid variability introduced when using different cell populations for each time point as required in luminometer-based luciferase detection or flow cytometry (for fluorescent reporters). Additionally, firefly luciferase has a short half-life of ∼2 h, so that its level should change concomitantly with the level of mRNA (25,26). This enables the use of bioluminescent imaging of luciferase protein activity as an indicator of mRNA transcript degradation by the delivered siRNA molecules.

Effect of siRNA dose on luciferase knockdown *in vitro*

The amount of siRNA applied to the extracellular media has a significant impact on the magnitude of the gene silencing but a

Table 2. Model parameters

Name	Description (units)	Determination	Value
max	Maximum number of cells (#)	Determined experimentally	*Fit to each system*
partition	Effective fraction of dose available to target cells	Estimated from experimental data	1×10^{-3}
rtot	Total available amount of RISC protein complexes (# L^{-1})	Literature (42–44)	1.9×10^{15}
Ve	Extracellular volume (L)	Specified experimentally *in vitro*, Estimated from experimental data and literature (45,46)	2×10^{-4} *1×10^{-5}*
Vi	Intracellular volume (L)	Literature (47)	4×10^{-12}
Vp	Plasma volume, mouse (L)	Literature (48)	1.5×10^{-3}
kbloodbind	Complex binding to blood components (h^{-1})	Estimated from experimental data	1×10^{-4}
kblooddis	Complex dissociation from blood components (h^{-1})	Estimated from experimental data	1×10^{-2}
kcleavage	Cleavage of target mRNA by activated RISC complex (h^{-1})	Literature (44)	7.2
kdegendna	Endosomal siRNA degradation (h^{-1})	Literature (32–34,49)	5×10^{-1}
kdeginna	Intracellular siRNA degradation (h^{-1})	Estimated from experimental data and literature (33)	2.9×10^{-2}
kdegmRNA	Target mRNA degradation (h^{-1})	Literature (50–53)	2
kdegprot	Target protein degradation, Luciferase (h^{-1})	Literature (25)	3.5×10^{-1}
kdegRISC	Activated RISC complex degradation (h^{-1})	Estimated from experimental data	7.7×10^{-2}
kdisRISC	Dissociation of activated RISC complex (h^{-1})	Chosen to be negligible once activated RISC is formed	1×10^{-9}
kdisRISCm	Dissociation of activated RISC complex and target mRNA (h^{-1})	Literature (42–44)	1
kelimec	Extracellular complex degradation (h^{-1})	Estimated from experimental data	8.7×10^{-2} *2.9×10^{-2}*
kelimpl	Plasma complex degradation (h^{-1})	Estimated from experimental data	5.8×10^{-2}
kescendna	Endosomal escape for siRNA (h^{-1})	Estimated from experimental data and literature (54)	6×10^{-2}
kescendvec	Endosomal escape for complex (h^{-1})	Estimated from experimental data and literature (54)	1×10^{-2}
kformmRNA	Formation of target mRNA (# L^{-1} h^{-1})	Literature (50,51)	5.2×10^{13}
kformprot	Formation of target protein (h^{-1})	Literature (50,51)	5.2×10^{2}
kformRISC	Formation of activated RISC complex (L #$^{-1}$ h^{-1})	Estimated from experimental data	2×10^{-19}
kformRISCm	Formation of activated RISC/mRNA complex (L #$^{-1}$ h^{-1})	Literature (42–44)	1.1×10^{14}
kgrowth	Cell growth rate (h^{-1})	Determined experimentally	*Fit to each system*
kint	Internalization (h^{-1})	Literature (12,13,55)	1×10^{-5} *5×10^{-7}*
ktransblood	Transport from plasma to extracellular fluid (h^{-1})	Estimated from experimental data	1×10^{-2}
kunpackcyt	Cytosolic complex unpackaging (h^{-1})	Estimated from experimental data	5×10^{-1} *6×10^{-2}*
kunpackend	Endosomal complex unpackaging (h^{-1})	Estimated from experimental data	1×10^{-4} *1×10^{-3}*

For parameters common to both *in vitro* and *in vivo* applications, the *in vivo* parameter values are shown in italics below the *in vitro* parameter values.

minimal impact on the overall duration (Figure 2A). Using the baseline parameters given in Table 2, the mathematical model predicts the trends observed experimentally (Figure 2B). Similar trends are observed with these siRNA doses in other luciferase-expressing cell lines (data not shown).

Effect of cell doubling time on luciferase knockdown *in vitro*

The majority of studies examining the kinetics of siRNA-mediated gene silencing *in vitro* have used rapidly dividing cell lines that typically have doubling times of ~1 day. Using these cell lines, the silencing effect generally lasts for ~1 week (27,28). To investigate whether this duration of silencing is intrinsic to siRNA or a result of dilution due to cell division, siRNA-mediated gene silencing was monitored in four luciferase-expressing cell lines with different observed doubling times: Neuro2A-Luc (0.8 days), LNCaP-Luc (1.4 days), HeLa-Luc (1.6 days) and CCD-1074Sk-Luc (nondividing). The cells were plated in 24-well plates and transfected under identical conditions to enable direct observation of the effect of cell doubling time alone. The experimental results in Figure 3A reveal that the dilution effect from cell division

can alter the duration of gene silencing. Consistent with previous observations, the duration of gene silencing in rapidly growing cell lines is ~1 week; however, cell lines with slower doubling times show a corresponding increase in the duration of silencing. Figure 3B shows the predicted effect of cell doubling time when the experimental transfection parameters are input into the mathematical model. The model predictions confirm that the dilution effect due to cell doubling time alone can account for the decreased duration of gene silencing in dividing cells. It is interesting to note that the duration of gene silencing in nondividing cells is ~3 weeks. This duration is consistent with the kinetics observed in two previous reports looking at siRNA-mediated gene silencing in nondividing mammalian neurons and primary macrophages (29,30). In nondividing cells, the duration of gene silencing is not controlled by dilution from cell division but by the intrinsic stability of siRNA within the cell.

Kinetics of luciferase knockdown by siRNA in subcutaneous tumors

Many tumors exhibit rapid growth with doubling times on the order of only a few days, and the duration of gene silencing
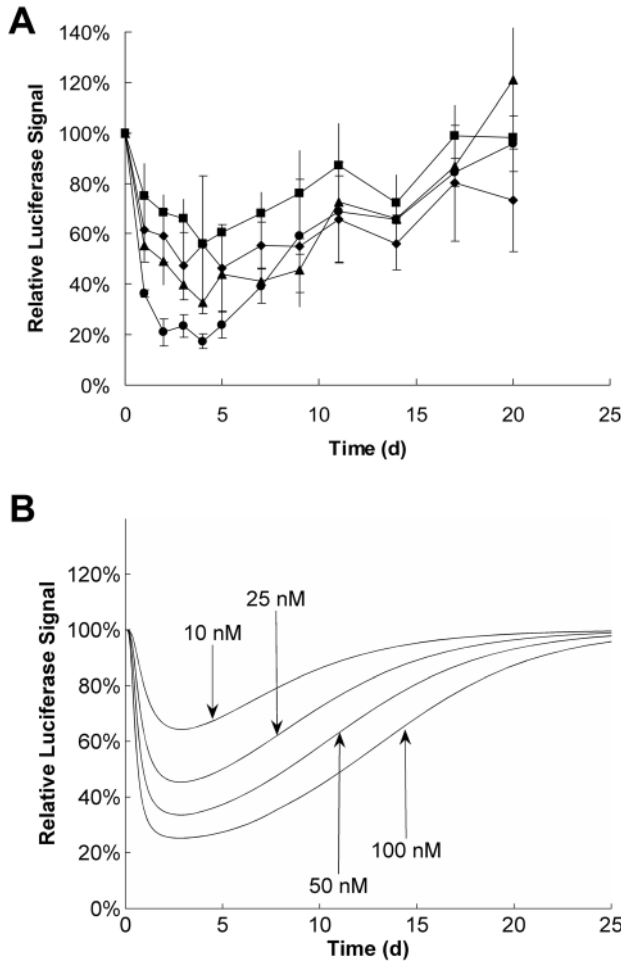
Figure 2. Effect of siRNA dose on the duration and magnitude of luciferase knockdown by siRNA in nondividing cells. (**A**) Experimental results using Oligofectamine to deliver siRNA to luciferase-expressing, nondividing fibroblasts with 1.5×10^5 cells per well in a 24-well plate. Data points represent the ratio of the average luciferase signal intensity from triplicate wells receiving siGL3 and siCON1 on day 0. Squares, 10 nM; diamonds, 25 nM; triangles, 50 nM; circles, 100 nM. (**B**) Luciferase knockdown after siRNA transfection predicted by the mathematical model using the baseline *in vitro* parameters given in Table 2 with the number of cells held constant at 1.5×10^5, a transfection time of 5 h, and a transfection efficiency of 90%.

Figure 3. Effect of cell doubling time on the duration of luciferase knockdown by siRNA *in vitro*. (**A**) Experimental results using Oligofectamine to deliver 100 nM siRNA to luciferase-expressing cells with a range of doubling times (dt). Data points represent the ratio of the average luciferase signal intensity from triplicate wells receiving siGL3 and siCON1 on day 0. Squares, Neuro2A-Luc (dt = 0.8 d); diamonds, LNCaP-Luc (dt = 1.4 d); triangles, HeLa-Luc (dt = 1.6 d); circles, CCD-1074Sk-Luc (nondividing). (**B**) Luciferase knockdown after siRNA transfection predicted by the mathematical model using the baseline *in vitro* parameters given in Table 2 with the initial number of dividing and nondividing cells equal to 5×10^4 and 1.5×10^5, respectively, a transfection time of 5 h, and a transfection efficiency of 90%.

should be limited by this rapid cell division. To test this hypothesis, subcutaneous tumors were created in A/J mice using luciferase-expressing Neuro2A-Luc cells. Since the goal was to observe the kinetics of gene silencing and not an actual therapeutic effect on the growth rate of the cells, siRNA against the luciferase gene (siGL3) and a control siRNA (siCON1) were used to show the sequence-specificity of the luciferase knockdown. Each mouse received three consecutive daily LPTV injections of transferrin-targeted polyplexes containing 2.5 mg/kg siRNA. After quantifying the luciferase activity in each tumor using the Xenogen camera, data were used to create a predicted logistic growth curve (Figure 4A). Because the siRNA targets only the luciferase gene, the growth rate of the cells should be unaffected; as a result, a decrease in luciferase signal intensity indicates a change in the luciferase protein level. Normalization to predicted growth curves allowed estimation of the knockdown resulting from siRNA treatment (Figure 4B).
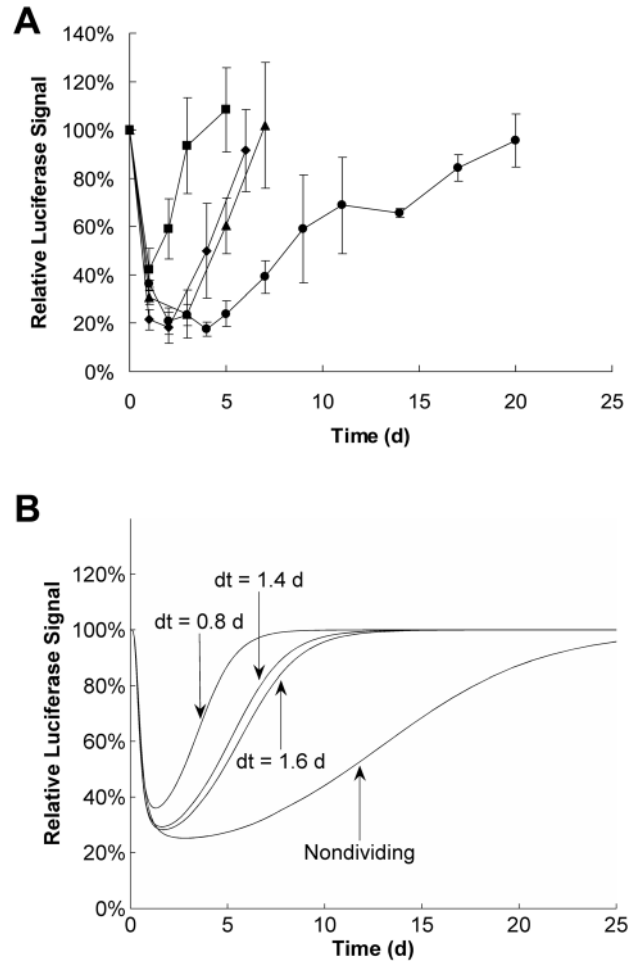
By adjusting only the parameters for the circulation/extracellular transport of the siRNA polyplexes, very good agreement was obtained between the model's predictions and the experimental data. The observed knockdown duration after three consecutive injections was around 10 days, consistent with the *in vitro* data for cell lines with similar observed growth rates.

Kinetics of luciferase knockdown by siRNA in hepatocytes

While cells in subcutaneous tumors are dividing rapidly (e.g. once per day), most of the hepatocytes in a normal mouse liver are in a state of growth arrest (31). Therefore, it was hypothesized that gene silencing by siRNA would exhibit different kinetics in hepatocytes versus tumors. Each BALB/c mouse received a single HPTV injection of 0.25 mg/kg plasmid and
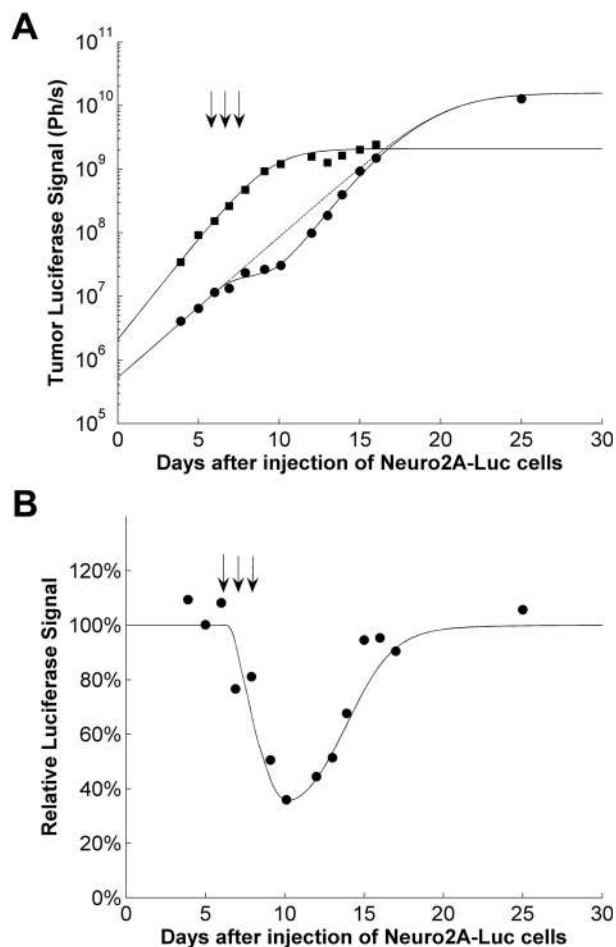
Figure 4. Kinetics of luciferase knockdown by siRNA in Neuro2A-Luc subcutaneous tumors in A/J mice. (**A**) Experimental and predicted results for luciferase knockdown after three consecutive LPTV injections on days 6, 7 and 8 of transferrin-targeted CDP-Im polyplexes containing 50 μg siRNA per 20 g mouse. Experimental data points are shown for a mouse receiving siCON1 (squares) and a mouse receiving siGL3 (circles). Solid lines represent the predicted luciferase signal with siRNA treatment and dashed lines represent the predicted luciferase signal in the absence of siRNA treatment. (**B**) Normalization of the observed luciferase signal in the siGL3-treated mouse to the predicted luciferase signal in the absence of treatment. Circles indicate the normalized experimental data points, while the solid line represents the response predicted by the mathematical model using the baseline *in vivo* parameters given in Table 2 and assuming that 50% of the total cells are reached with each dose.

2.5 mg/kg siGL3 on day 0, and the Xenogen camera was used to follow the luciferase signal in each mouse liver. Normalization to the signal intensity in mice that received plasmid only (no siRNA) allowed quantification of the percent knockdown by siRNA. Figure 5 shows the experimental data together with the model predictions. Similar to the *in vitro* results for gene silencing in nondividing cells, the duration of gene silencing lasts for ∼3–4 weeks in the hepatocytes after a single dose of siRNA.

Effect of siRNA stability on luciferase knockdown by siRNA

Because both double-stranded and single-stranded nucleic acids are rapidly degraded in serum, current efforts in the
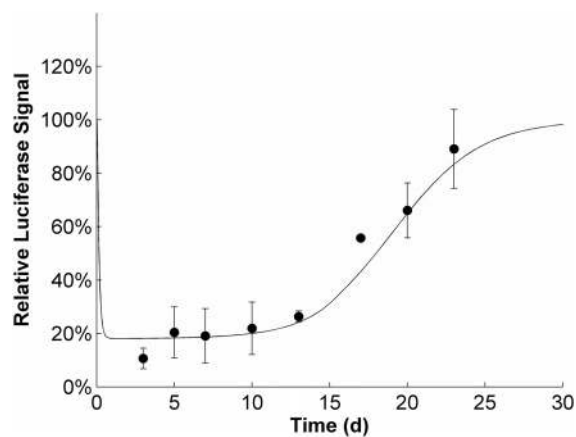

Figure 5. Kinetics of luciferase knockdown by siRNA in nondividing hepatocytes in BALB/c mice. Experimental and predicted results are shown for luciferase knockdown after hydrodynamic tail-vein co-injection of 5 μg pApoEHCRLuc and 50 μg siRNA per 20 g mouse on day 0. Circles represent the ratio of the average luciferase signal intensity from three mice receiving plasmid + siRNA to the luciferase signal intensity from three mice receiving plasmid alone. The predicted luciferase knockdown, given by the solid line, was calculated using the baseline *in vivo* parameters given in Table 2 with the following modifications to account for hydrodynamic injection of naked siRNA without a delivery vehicle: eliminate steps involving the complexes (*kescendvec*, *kunpackend*, *kunpackcyt*), modify uptake and intracellular trafficking to match observed kinetics (*partition* = 1×10^{-2}, *ktransblood* = 1, *kint* = 1×10^{-3} h^{-1}, *kescendna* = 1×10^{-2} h^{-1}, *kdegendna* = 5×10^{-3} h^{-1}), and modify extracellular volume (*Ve* = 1.5×10^{-5} L). The *kescendna* and *kdegendna* may no longer represent endosomal processes as hydrodynamically injected naked siRNA may be internalized through different vesicles or partitioned into a separate intracellular compartment (e.g. nucleus) that exhibits different degradation and release kinetics than in standard or receptor-mediated endocytosis of siRNA-containing complexes. The total number of hepatocytes was chosen to be 5×10^{7}, on the same order of magnitude as the number of hepatocytes in a mouse liver (40,41).

field of nucleic acid-based therapeutics seek to enhance the stability of the nucleic acids with the goal of increasing the duration of gene silencing by boosting their bioavailability and possibly prolonging their persistence intracellularly (32–34). Layzer and co-workers studied the kinetics of gene silencing in HeLa cells using 2′-F-modified siRNA and unmodified 2′-OH siRNA. Although the 2′-F-modified siRNA led to a significant increase in serum stability, it appeared to have no effect on the duration of gene silencing after transfection. This suggests that the intracellular stability of siRNA molecules is not the limiting factor controlling the duration of gene silencing in rapidly dividing cells; instead, dilution due to cell division limits how long gene silencing can occur under these conditions. If the intracellular half-life of siRNA molecules is already around 24 h, then even modifications to increase the half-life to >72 h have an insignificant effect on the duration of gene silencing (Figure 6). These model predictions corroborate the experimental results obtained by Layzer and co-workers (33). On the other hand, the outcome of using modified siRNA may be different in slowly dividing or nondividing cells since the intracellular siRNA half-life will be shorter than the cell doubling time, meaning dilution due to cell division will no longer be the dominant factor. Increasing the persistence of siRNA within the cell might prolong the duration of gene silencing. Results from such studies in nondividing cells should be interpreted carefully since the apparent intracellular stability of
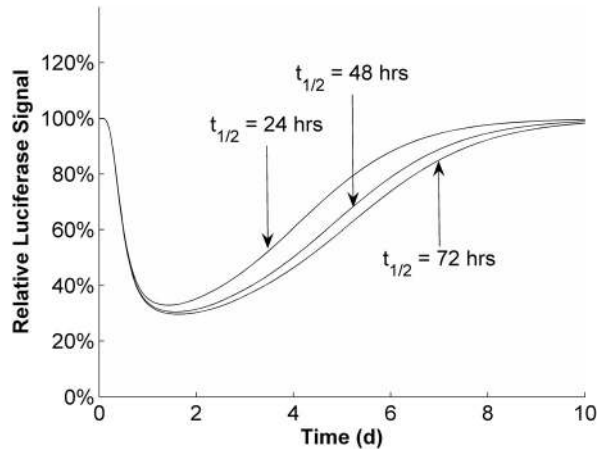
Figure 6. Effect of intracellular siRNA half-life on the duration of siRNA-mediated gene silencing *in vitro*. Curves represent model predictions for luciferase knockdown after transfection with 100 nM siRNA against luciferase on day 0 with a cell doubling time of 1 day ($kgrowth = 0.0029$ h^{-1}) and intracellular siRNA half-lives of 24, 48 and 72 h ($kdeginna = 0.029$, 0.014 and 0.01 h^{-1}). The initial number of cells was 5×10^4, transfection time was 5 h, transfection efficiency was 90%, and all other parameters were kept at their baseline *in vitro* values given in Table 2.

siRNA molecules may be caused by association with other intracellular components or localization to specific compartments, both of which could lead to degradation kinetics independent of the properties of the siRNA molecules alone. In that case, modified siRNA would not necessarily increase the duration of gene silencing relative to unmodified siRNA even in nondividing cells.

Multiple doses to prolong luciferase knockdown by siRNA in nondividing cells

The previous studies have looked at the transient knockdown of the luciferase reporter gene by 1–3 injections of siRNA over a short-term period; even in nondividing cells, the maximum duration of silencing using typical siRNA doses is ∼3–4 weeks. However, a clinically relevant treatment regimen using siRNA may require that a gene be silenced for a prolonged period of time. Some have attempted to solve this problem by using lentiviral delivery of expressed short-hairpin siRNAs (shRNAs) to achieve sustained gene silencing *in vitro* and *in vivo* (35,36). Precise control of the intracellular level of siRNA and having a means to turn off its production when treatment is no longer necessary represent two major challenges to this use of shRNA. On the other hand, the intrinsically transient nature of siRNAs makes them more amenable to disease treatments in which the treatment is given over a period of time and then stopped once the desired therapeutic outcome (e.g. regression of a tumor or inhibition of viral growth) is achieved. To illustrate how properly timed doses of siRNA can prolong gene silencing by siRNA, nondividing CCD-1074Sk-Luc cells were transfected with a second dose of siRNA 4 days after the initial dose (Figure 7A). With a second dose of 100 nM siRNA, the luciferase protein levels remained at <40% of the steady-state value for an additional 4 days. If the trends continue in such a fashion, a 100 nM dose every 4 days could lead to persistent gene silencing as shown by model calculations in Figure 7B.
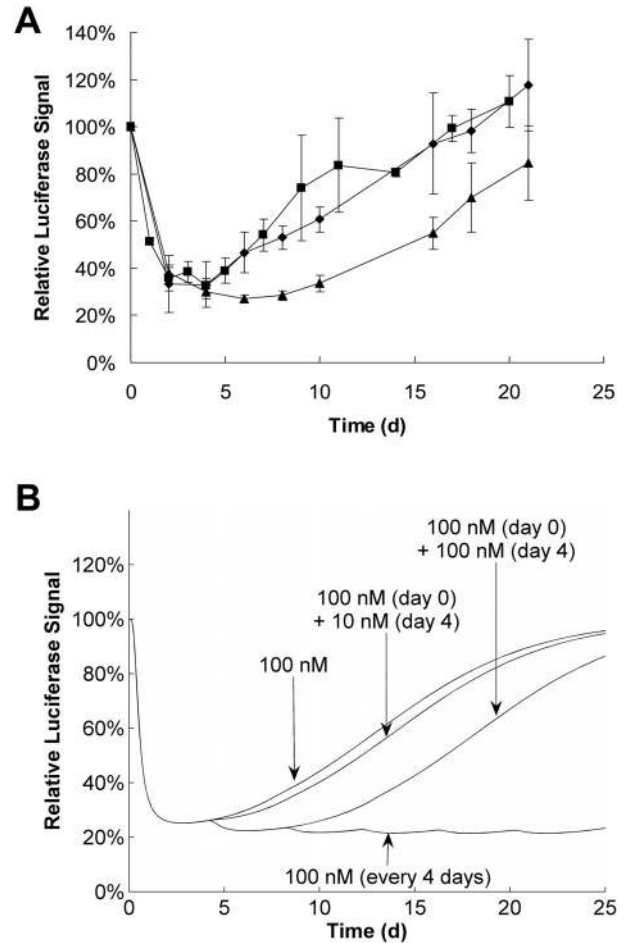

Figure 7. Effect of siRNA dose frequency on the duration of luciferase knockdown by siRNA in nondividing cells. (**A**) Experimental results using Oligofectamine to deliver siRNA to luciferase-expressing nondividing fibroblasts *in vitro*. Data points represent the ratio of the average luciferase signal intensity from triplicate wells receiving siGL3 and siCON1. To facilitate comparison of the knockdown kinetics, the data points are normalized such that all three curves exhibit the same magnitude of knockdown for the first four days since all three received the same treatment over this period. This normalization permits comparison of the kinetics of gene silencing observed with different treatments even though the absolute magnitude of the knockdown varied slightly in each experiment. Squares, 100 nM (day 0); diamonds, 100 nM (day 0) + 10 nM (day 4); triangles, 100 nM (day 0) + 100 nM (day 4). (**B**) Luciferase knockdown after siRNA transfection predicted by the mathematical model using the baseline *in vitro* parameters given in Table 2 with the number of cells equal to 1.5×10^5, a transfection time of 5 h, and a transfection efficiency of 90%.

Considerations for siRNA-based treatments that require a threshold knockdown for efficacy

Because siRNA treatment of rapidly dividing cells requires treating more cells over time while also having to deal with dilution effects, the amount of target gene or protein knockdown will be less than that observed in slowly dividing or nondividing cells. More frequent dosing is required to overcome these barriers. Cancer is one example of a disease often characterized by rapid cell division that may require target gene knockdown lasting longer than that which can be achieved with a single dose of siRNA. To address this situation, the mathematical model was used to estimate siRNA dosing schedules needed to maintain a given gene below a

threshold value for an extended period of time in dividing cells. While the magnitude of target gene (or protein) reduction or the duration of knockdown relative to the steady-state value in the absence of treatment can be relatively good indicators of the success of an siRNA treatment, the therapeutic efficacy of an siRNA treatment regimen should perhaps be judged by the length of time it is able to maintain the target gene or protein level below a given threshold. Although a short, substantial knockdown of certain targets may be sufficient to trigger a cascade of downstream effects, other situations may require considerably longer knockdown to achieve the desired therapeutic effect. Additionally, this therapeutic effect may only be seen when the target protein is reduced below a threshold, or some fraction of its pre-treatment value.

The data in Figure 8 show how the mathematical model can be used to simulate the effects of cell doubling time and target protein half-life during treatment with siRNA. To avoid unnecessary complications, the calculations ignore the circulation/extracellular transport and consider each siRNA dose already in the local extracellular environment of the cells (analogous to the *in vitro* situation). Figure 8A–D gives results that demonstrate how target protein half-life can impact the observed dynamics of protein knockdown with once- or twice-weekly dosing in rapidly dividing or nondividing cells. For a target protein with a short half-life in rapidly dividing cells, even twice-weekly dosing still can result in significant oscillations which may hinder the ability to cause a phenotypic change in the target cells (Figure 8A). If the target protein has a long half-life, then twice-weekly dosing is able to maintain steady knockdown at ∼50% of the steady-state level, but this magnitude of protein knockdown is not achieved until about a week after the first dose of siRNA (Figure 8B). In nondividing cells, once-weekly dosing is adequate to maintain persistent silencing at ∼20% of the steady-state value (Figure 8C and D). Again, this protein knockdown can only be achieved after more than a week from the initial siRNA dose if the target protein half-life is very long (Figure 8D). The fraction of the total treatment time during which a target protein is below a threshold (e.g. 50% steady-state value) can be used as a metric to compare the efficacy of different treatment regimens. The data illustrated in Figure 8E reveal how cell growth rate and target protein half-life can affect protein knockdown when siRNA is administered once on day 0, once-weekly or twice-weekly over the 25-day treatment. As expected, cell growth rate has a large impact on the duration of knockdown, directly affecting the fraction of the total time that the target protein level can be reduced below the threshold of 50%.

DISCUSSION

A more thorough understanding of the factors affecting the kinetics of siRNA-mediated gene silencing should prove to be invaluable for experimental and clinical applications of siRNA. Given the relatively recent discovery of RNAi, details of its action are still being elucidated, and many of the current siRNA dosing schedules used in literature are based on precedence rather than being optimized for each system. The high cost of siRNA molecules, especially for *in vivo* studies, limits systematic exploration of the parameter space needed to achieve the most effective siRNA dosing schedule for each model system. This situation can be partially rectified by using mathematical modeling to give insights that help direct experimental studies. Here, we employed bioluminescent imaging and mathematical modeling to investigate the effects of target-specific and treatment-specific parameters on siRNA-mediated gene silencing *in vitro* and *in vivo*.

The experimental data presented here show the effects of cell doubling time, siRNA dosing schedule, and siRNA delivery method on luciferase reporter-protein knockdown and aid in developing mathematical models of siRNA delivery to and function within mammalian cells. Luciferase knockdown in cell lines engineered to constitutively express luciferase was used to mimic the knockdown of an endogenously expressed gene, analogous to an oncogene whose presence in a cell can lead to tumorigenicity. The luciferase-expressing cell lines were used in cell culture experiments or injected into mice and then monitored for luciferase expression using noninvasive bioluminescent imaging with the Xenogen Imaging System. The duration of gene silencing lasted for ∼1 week in rapidly dividing cells but longer than 3 weeks in nondividing cells both *in vitro* and *in vivo*, supporting the hypothesis that dilution due to cell division is the major factor controlling the duration of luciferase knockdown in rapidly dividing cells.

The duration of gene silencing by siRNA can be longer than that achieved with other nucleic acid-based gene inhibition strategies, such as antisense, whose knockdown typically lasts only on the order of 1–2 days. Bertrand and co-workers (37) studied antisense- and siRNA-mediated inhibition of GFP in HeLa cells and showed that while antisense-mediated inhibition diminished after only 1 day, the siRNA-mediated inhibition was still increasing. This significant difference in the duration of gene silencing could become important when trying to use either antisense or siRNA molecules as therapeutic agents. In fact, the short duration of gene silencing by certain nucleic acid-based gene inhibition strategies could preclude their ability to alter cellular behavior if the target gene is not silenced for an adequate amount of time. This would be particularly apparent if the target protein has a long intracellular half-life; then, knockdown of the target mRNA may not result in target protein knockdown if the mRNA levels can be restored before a significant amount of protein has degraded.

The findings presented here highlight several key considerations for experimental design when evaluating the efficacy of siRNA against certain genes that produce proteins with long half-lives. If the knockdown phenotype does not become apparent until the protein is below a certain threshold, then observation at early time points may not reveal any effect. This is crucial for *in vitro* studies aimed at testing the ability of a therapeutic siRNA to induce apoptosis or growth arrest in certain cell lines. Common practice is to look at time points within 48 and 72 h; here, model predictions suggest that these time points may be too early if the target protein half-life is any longer than a couple of days. Similar considerations should be made when deciding dosing schedules for *in vivo* studies using siRNA for protein knockdown in tumors (e.g. an oncogenic fusion protein), since proteins with longer half-lives will show a slower initial response to the therapy but will require less frequent dosing for persistent silencing. An important area for future research will be to determine to what extent a gene or protein needs to be knocked down before the intended therapeutic effect is realized. Such information can be combined with mathematical models like the one presented here to more
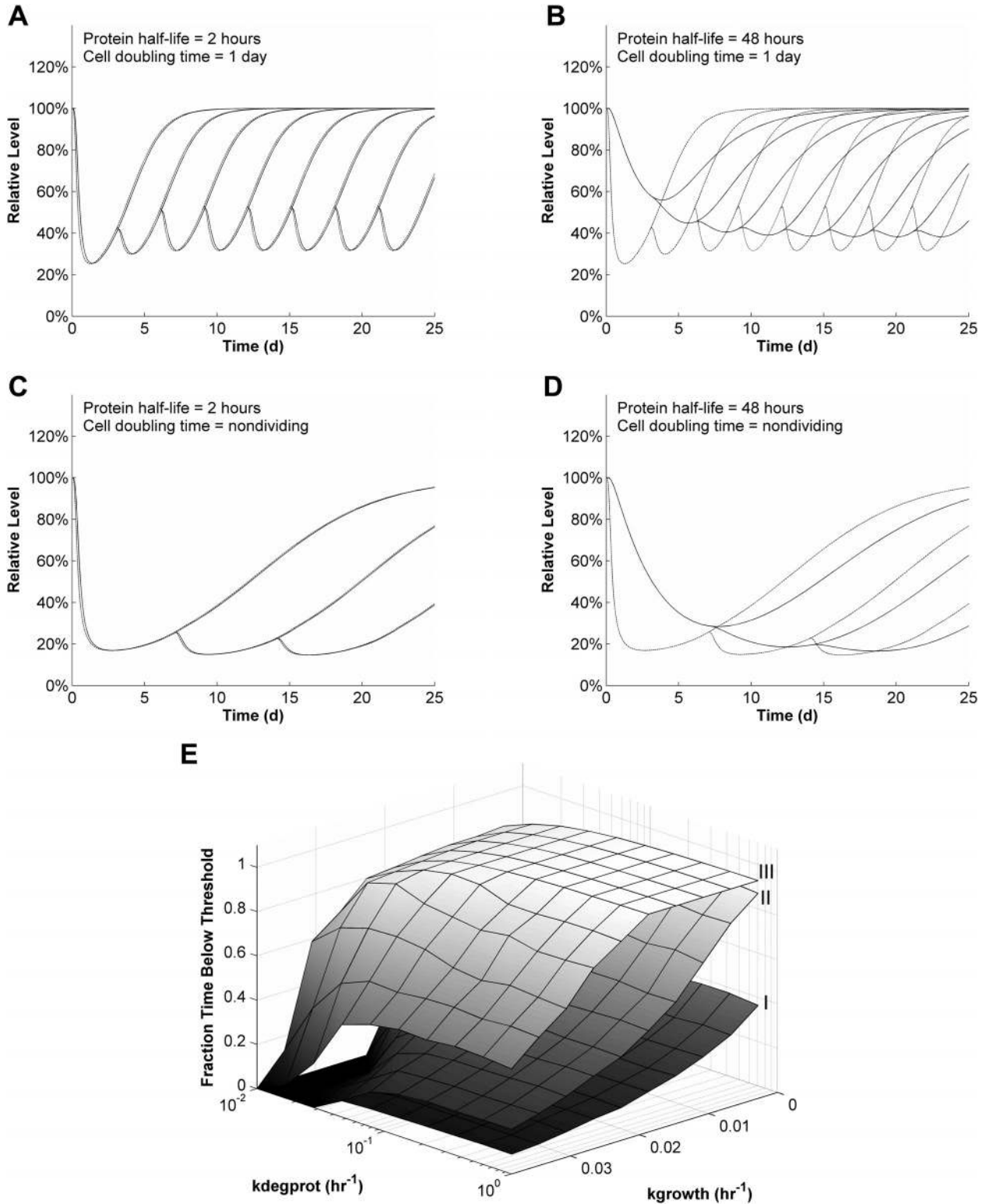
Figure 8. Effect of cell doubling time and target protein half-life on the ability to maintain persistent gene silencing. All plots represent predicted mRNA (dashed lines) and protein (solid lines) knockdown in transfected cells using the baseline *in vitro* parameters given in Table 2, a transfection time of 5 h, and an initial number of dividing and nondividing cells equal to 5×10^4 and 1.5×10^5, respectively. (**A**) Dose of 100 nM siRNA every 3 days with a target protein half-life of 2 h (*kdegprot* = 0.35 h^{-1}) in cells with a doubling time of 1 day (*kgrowth* = 0.029 h^{-1}). (**B**) Dose of 100 nM siRNA every 3 days with a target protein half-life of 48 h (*kdegprot* = 0.014 h^{-1}) in cells with a doubling time of 1 day (*kgrowth* = 0.029 h^{-1}). (**C**) Dose of 100 nM siRNA every 7 days with a target protein half-life of 2 h (*kdegprot* = 0.35 h^{-1}) in nondividing cells. (**D**) Dose of 100 nM siRNA every 7 days with a target protein half-life of 48 h (*kdegprot* = 0.014 h^{-1}) in nondividing cells. (**E**) Effect of variations in cell doubling time and target protein half-life on the ability to maintain a target protein level below a threshold of 50% its pre-treatment value over the 25-day period. **I**, 100 nM (day 0); **II**, 100 nM (days 0, 7, 14); **III**, 100 nM (days 0, 3, 7, 10, 14, 17, 21, 24). Surface vertices represent the fraction of the total time during which the relative protein level is below the 50% threshold.

accurately determine the required treatment regimen needed to achieve efficacy. Although the model in its current form does not allow for treatment effects other than target gene knockdown, the simple addition of a death parameter to the cell growth equation could provide a target cell death rate that depends on the reduction of the target protein level below a certain threshold. Other slightly more complicated modifications to the current set of equations could incorporate recruitment of immune effector cells, effects on angiogenesis or even sensitization to other treatments including chemotherapy.

While the mathematical model can predict many of the trends observed experimentally for the systems used here, confidence in the actual magnitude and duration of the predicted gene silencing in hypothetical situations can still be greatly increased as more accurate parameter values become available. Parametric sensitivity analysis was performed using the SENS_SYS modification of the ODE15s solver in MATLAB. Parameters governing RISC formation (*kformRISC*) and binding to target mRNA (*kformRISCm*) have a significant impact on target mRNA or protein levels. Although studies of the RISC complex are rapidly elucidating details of its mechanism and kinetics, these parameters will need to be refined as more data become available. Additional equations will be needed to model a multi-step RISC formation process, or the lumped rate constants currently used can be modified to provide reasonable estimates of the overall kinetics. As expected, target mRNA and protein levels are also sensitive to parameters governing the siRNA delivery process, such as cellular uptake, endosomal escape and vector unpackaging. It will be important to determine these parameters for each individual delivery vehicle since such rates will vary from system to system. With knowledge of these different parameters, the model can be used to mimic delivery by a variety of methods including naked siRNA (by high-pressure or low-pressure tail-vein injection) or formulation into liposomes, lipoplexes or polyplexes. Such comparisons may reveal how the characteristics of each delivery method specifically affect the kinetics of gene silencing. This information may help to focus design improvements for delivery vehicles or improve the efficacy of treatment regimens employing them, as suggested in general for gene delivery by Varga and co-workers (38). Of the parameters intrinsic to the target cells, the most important are the cell growth rate (dilution effect), compartment volumes (that control the concentration of siRNA available to drive uptake or association processes), and the stability of the target mRNA and protein molecules. The current set of model equations predicts that the stability of the mRNA transcript has a greater effect on the magnitude and duration of gene silencing than the absolute transcript number. This is because the relative knockdown is controlled largely by the relative sizes of the two mRNA degradation terms: natural turnover within the cell and degradation by RNAi. Therefore, the contribution from RNAi leads to greater deviation from the steady-state mRNA level for more stable mRNA molecules. Similar reasoning can be applied to other gene inhibition strategies, such as antisense, that act at the mRNA level (39).

Based on these findings and the literature to date, siRNA appears to be the most potent and effective nucleic acid-based therapeutic aimed at post-transcriptional gene silencing. The siRNA molecules can achieve >80% target protein inhibition at nanomolar concentrations, and their enhanced intracellular

stability enables knockdown that can last for weeks in nondividing cells. It is shown here that an optimized siRNA-based treatment schedule can be designed to achieve prolonged gene silencing by properly timed injections of siRNA. Mathematical modeling can help to realize these optimized treatments at a fraction of the time and cost that would be required by experimentation alone. Although there is no substitute for experimental data, especially for highly variable and not completely definable biological systems, model calculations can help to guide effective experimental design and aid in data interpretation. With the burgeoning interest in nucleic acid-based therapeutics such as siRNA, development of mathematical models such as the one presented here may expedite their translation into clinically relevant therapeutics for disease treatment and management.

SUPPLEMENTARY DATA

Supplementary Data are available at NAR Online.

REFERENCES

1. Fire,A., Xu,S., Montgomery,M.K., Kostas,S.A., Driver,S.E. and Mello,C.C. (1998) Potent and specific genetic interference by double-stranded RNA in *Caenorhabditis elegans*. *Nature*, **391**, 806–811.
2. Medema,R.H. (2004) Optimizing RNA interference for application in mammalian cells. *Biochem. J.*, **380**, 593–603.
3. Mittal,V. (2004) Improving the efficiency of RNA interference in mammals. *Nature Rev. Genet.*, **5**, 355–365.
4. Sioud,M. (2005) On the delivery of small interfering RNAs into mammalian cells. *Expert Opin. Drug Deliv.*, **2**, 639–651.
5. Ryther,R., Flynt,A., Phillips,J.,III and Patton,J. (2005) siRNA therapeutics: big potential from small RNAs. *Gene Ther.*, **12**, 5–11.
6. Hannon,G.J. and Rossi,J.J. (2004) Unlocking the potential of the human genome with RNA interference. *Nature*, **431**, 371–378.
7. Dorsett,Y. and Tuschl,T. (2004) siRNAs: applications in functional genomics and potential as therapeutics. *Nature Rev. Drug Discov.*, **3**, 318–329.
8. Caplen,N.J. and Mousses,S. (2003) Short interfering RNA (siRNA)-mediated RNA interference (RNAi) in human cells. *Ann. NY Acad. Sci.*, **1002**, 56–62.
9. Elbashir,S.M., Harborth,J., Lendeckel,W., Yalcin,A., Weber,K. and Tuschl,T. (2001) Duplexes of 21-nucleotide RNAs mediate RNA interference in cultured mammalian cells. *Nature*, **411**, 494–498.

10. Scherer,L.J. and Rossi,J.J. (2003) Approaches for the sequence-specific knockdown of mRNA. *Nat. Biotechnol.*, **21**, 1457–1465.

11. Stark,G.R., Kerr,I.M., Williams,B.R.G., Silverman,R.H. and Schreiber,R.D. (1998) How cells respond to interferons. *Annu. Rev. Biochem.*, **67**, 227–264.

12. Overhoff,M., Wunsche,W. and Sczakiel,G. (2004) Quantitative detection of siRNA and single-stranded oligonucleotides: relationship between uptake and biological activity of siRNA. *Nucleic Acids Res.*, **32**, e170.

13. Lingor,P., Michel,U., Scholl,U., Bahr,M. and Kugler,S. (2004) Transfection of 'naked' siRNA results in endosomal uptake and metabolic impairment in cultured neurons. *Biochem. Biophys. Res. Commun.*, **315**, 1126–1133.

14. Hu-Lieskovan,S., Heidel,J.D., Bartlett,D.W., Davis,M.E. and Triche,T.J. (2005) Sequence-specific knockdown of EWS-FLI1 by targeted, nonviral delivery of small interfering RNA inhibits tumor growth in a murine model of Ewing's sarcoma. *Cancer Res.*, **65**, 8984–8992.

15. Bergstrom,C.T., McKittrick,E. and Antia,R. (2003) Mathematical models of RNA silencing: Unidirectional amplification limits accidental self-directed reactions. *Proc. Natl Acad. Sci. USA*, **100**, 11511–11516.

16. Groenenboom,M.A.C., Maree,A.F.M. and Hogeweg,P. (2005) The RNA silencing pathway: the bits and pieces that matter. *PLoS Comput. Biol.*, **1**, 155–165.

17. Raab,R.M. and Stephanopoulos,G. (2004) Dynamics of gene silencing by RNA interference. *Biotechnol. Bioeng.*, **88**, 121–132.

18. Arciero,J.C., Jackson,T.L. and Kirschner,D.E. (2004) A mathematical model of tumor-immune evasion and siRNA treatment. *Discrete and Continuous Dynamical Systems*, **4**, 39–58.

19. Bahner,I., Kearns,K., Hao,Q., Smogorzewska,E. and Kohn,D. (1996) Transduction of human CD34+ hematopoietic progenitor cells by a retroviral vector expressing an RRE decoy inhibits human immunodeficiency virus type 1 replication in myelomonocytic cells produced in long-term culture. *J. Virol.*, **70**, 4352–4360.

20. Challita,P.-M., Skelton,D., El-Khoueiry,A., Yu,X.-J., Weinberg,K. and Kohn,D.B. (1995) Multiple modifications in cis elements of the long terminal repeat of retroviral vectors lead to increased expression and decreased DNA methylation in embryonic carcinoma cells. *J. Virol.*, **69**, 748–755.

21. Davis,M.E., Pun,S.H., Bellocq,N.C., Reineke,T.M., Popielarski,S.R., Mishra,S. and Heidel,J.D. (2004) Self-assembling nucleic acid delivery vehicles via linear, water-soluble cyclodextrin-containing polymers. *Curr. Med. Chem.*, **11**, 1241–1253.

22. Pun,S.H. and Davis,M.E. (2002) Development of a nonviral gene delivery vehicle for systemic application. *Bioconjug. Chem.*, **13**, 630–639.

23. Kobayashi,N., Nishikawa,M., Hirata,K. and Takakura,Y. (2004) Hydrodynamics-based procedure involves transient hyperpermeability in the hepatic cellular membrane: implication of a nonspecific process in efficient intracellular gene delivery. *J. Gene. Med.*, **6**, 584–592.

24. Andrianaivo,F., Lecocq,M., Wattiaux-De Coninck,S., Wattiaux,R. and Jadot,M. (2004) Hydrodynamics-based transfection of the liver: entrance into hepatocytes of DNA that causes expression takes place very early after injection. *J. Gene. Med.*, **6**, 877–883.

25. Ignowski,J.M. and Schaffer,D.V. (2004) Kinetic analysis and modeling of firefly luciferase as a quantitative reporter gene in live mammalian cells. *Biotechnol. Bioeng.*, **86**, 827–834.

26. Sweeney,T.J., Mailander,V., Tucker,A.A., Olomu,A.B., Zhang,W., Cao,Y.-a., Negrin,R.S. and Contag,C.H. (1999) Visualizing the kinetics of tumor-cell clearance in living animals. *Proc. Natl Acad. Sci. USA*, **96**, 12044–12049.

27. Novina,C.D., Murray,M.F., Dykxhoorn,D.M., Beresford,P.J., Riess,J., Lee,S.-K., Collman,R.G., Lieberman,J., Shankar,P. and Sharp,P.A. (2002) siRNA-directed inhibition of HIV-1 infection. *Nature Med.*, **8**, 681–686.

28. Tuschl,T. (2002) Expanding small RNA interference. *Nat. Biotechnol.*, **20**, 446–448.

29. Song,E., Lee,S.-K., Dykxhoorn,D.M., Novina,C., Zhang,D., Crawford,K., Cerny,J., Sharp,P.A., Lieberman,J., Manjunath,N. *et al.* (2003) Sustained small interfering RNA-mediated human immunodeficiency virus type I inhibition in primary macrophages. *J. Virol.*, **77**, 7174–7181.

30. Omi,K., Tokunaga,K. and Hohjoh,H. (2004) Long-lasting RNAi activity in mammalian neurons. *FEBS Lett.*, **558**, 89–95.

31. Schibler,U. (2003) Circadian rhythms: liver regeneration clocks on. *Science*, **302**, 234–235.

32. Bertrand,J.-R., Pottier,M., Vekris,A., Opolon,P., Maksimenko,A. and Malvy,C. (2002) Comparison of antisense oligonucleotides and siRNAs in cell culture and *in vivo*. *Biochem. Biophys. Res. Commun.*, **296**, 1000–1004.

33. Layzer,J.M., McCaffrey,A.P., Tanner,A.K., Huang,Z., Kay,M.A. and Sullenger,B.A. (2004) *In vivo* activity of nuclease-resistant siRNAs. *RNA*, **10**, 766–771.

34. Elmén,J., Thonberg,H., Ljungberg,K., Frieden,M., Westergaard,M., Xu,Y., Wahren,B., Liang,Z., Ørum,H., Koch,T. *et al.* (2005) Locked nucleic acid (LNA) mediated improvements in siRNA stability and functionality. *Nucleic Acids Res.*, **33**, 439–447.

35. Tiscornia,G., Singer,O., Ikawa,M. and Verma,I.M. (2003) A general method for gene knockdown in mice by using lentiviral vectors expressing small interfering RNA. *Proc. Natl Acad. Sci. USA*, **100**, 1844–1848.

36. Rubinson,D.A., Dillon,C.P., Kwiatkowski,A.V., Sievers,C., Yang,L., Kopinja,J., Zhang,M., McManus,M.T., Gertler,F.B., Scott,M.L. *et al.* (2003) A lentivirus-based system to functionally silence genes in primary mammalian cells, stem cells and transgenic mice by RNA interference. *Nature Genet.*, **33**, 401–406.

37. Bertrand,J.-R., Pottier,M., Vekris,A., Opolon,P., Maksimenko,A. and Malvy,C. (2002) Comparison of antisense oligonucleotides and siRNAs in cell culture and *in vivo*. *Biochem. Biophys. Res. Commun.*, **296**, 1000–1004.

38. Varga,C., Tedford,N., Thomas,M., Klibanov,A., Griffith,L. and Lauffenburger,D. (2005) Quantitative comparison of polyethylenimine formulations and adenoviral vectors in terms of intracellular gene delivery processes. *Gene Ther.*, **12**, 1023–1032.

39. Roth,C.M. (2005) Molecular and cellular barriers limiting the effectiveness of antisense oligonucleotides. *Biophys. J.*, **89**, 2286–2295.

40. Kumaran,V., Benten,D., Follenzi,A., Joseph,B., Sarkar,R. and Gupta,S. (2005) Transplantation of endothelial cells corrects the phenotype in hemophilia A mice. *J. Thromb. Haemost.*, **3**, 2022–2031.

41. Rajvanshi,P., Kerr,A., Bhargava,K., Burk,R.D. and Gupta,S. (1996) Studies of liver repopulation using the dipeptidyl peptidase IV-deficient rat and other rodent recipients: Cell size and structure relationships regulate capacity for increased transplanted hepatocyte mass in the liver lobule. *Hepatology*, **23**, 482–496.

42. Martinez,J. and Tuschl,T. (2004) RISC is a 5′ phosphomonoester-producing RNA endonuclease. *Genes Dev.*, **18**, 975–980.

43. Haley,B. and Zamore,P.D. (2004) Kinetic analysis of the RNAi enzyme complex. *Nature Struct. Mol. Biol.*, **11**, 599–606.

44. Brown,K.M., Chu,C.-y. and Rana,T.M. (2005) Target accessibility dictates the potency of human RISC. *Nature Struct. Mol. Biol.*, **12**, 469–470.

45. Krol,A., Maresca,J., Dewhirst,M.W. and Yuan,F. (1999) Available volume fraction of macromolecules in the extravascular space of a fibrosarcoma: implications for drug delivery. *Cancer Res.*, **59**, 4136–4141.

46. Pathak,A.P., Artemov,D., Ward,B.D., Jackson,D.G., Neeman,M. and Bhujwalla,Z.M. (2005) Characterizing extravascular fluid transport of macromolecules in the tumor interstitium by magnetic resonance imaging. *Cancer Res.*, **65**, 1425–1432.

47. Chiu,D.T. and Zare,R.N. (1998) Assaying for peptides in individual *Aplysia* neurons with mass spectrometry. *Proc. Natl Acad. Sci. USA*, **95**, 3338–3340.

48. Hoff,J. (2000) Methods of Blood Collection in the Mouse. *Lab Animal*, **29**, 47–53.

49. Chiu,Y.-L. and Rana,T.M. (2003) siRNA function in RNAi: a chemical modification analysis. *RNA*, **9**, 1034–1048.

50. Alberts,B., Johnson,A., Lewis,J., Raff,M., Roberts,K. and Walter,P. (2002) *Molecular Biology of the Cell, 4 edn.* Garland Science, NY.

51. Stryer,L. (1995) *Biochemistry, 4 edn.* W. H. Freeman and Company, NY.

52. Velculescu,V.E., Madden,S.L., Zhang,L., Lash,A.E., Yu,J., Rago,C., Lal,A., Wang,C.J., Beaudry,G.A., Ciriello,K.M. *et al.* (1999) Analysis of human transcriptomes. *Nature Genet.*, **23**, 387–388.

53. Godfrey,T.E., Kim,S.-H., Chavira,M., Ruff,D.W., Warren,R.S., Gray,J.W. and Jensen,R.H. (2000) Quantitative mRNA expression analysis from formalin-fixed, paraffin-embedded tissues using 5′ nuclease quantitative reverse transcription-polymerase chain reaction. *J. Mol. Diagn.*, **2**, 84–91.

54. Varga,C.M., Hong,K. and Lauffenburger,D.A. (2001) Quantitative analysis of synthetic gene delivery vector design properties. *Mol. Ther.*, **4**, 438–446.

55. Banks,G.A., Roselli,R.J., Chen,R. and Giorgio,T.D. (2003) A model for the analysis of nonviral gene therapy. *Gene Ther.*, **10**, 1766–1775.